US Army Corps of Engineers

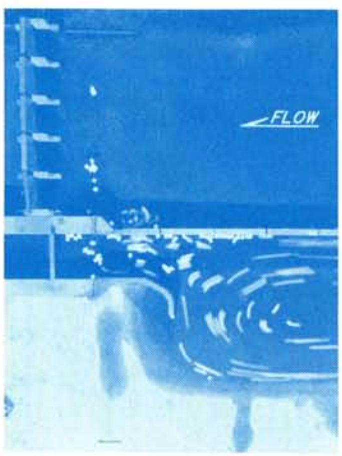

HYDRAULICS LABORATORY

TECHNICAL REPORT HL-91-14

A TURBULENCE MODEL FOR RECIRCULATING FLOW

by

Robert S. Bernard

Hydraulics Laboratory

DEPARTMENT OF THE ARMY
Waterways Experiment Station, Corps of Engineers
3909 Halls Ferry Road, Vicksburg, Mississippi 39180-6199

September 1991
Final Report

Approved For Public Release; Distribution Is Unlimited

Prepared for DEPARTMENT OF THE ARMY
Assistant Secretary of the Army (R&D)
Washington, DC 20310

REPORT DOCUMENTATION PAGE

Form Approved
OMB No. 0704-0188

1. AGENCY USE ONLY *(Leave blank)*

2. REPORT DATE
September 1991

3. REPORT TYPE AND DATES COVERED
Final report

4. TITLE AND SUBTITLE

A Turbulence Model for Recirculating Flow

5. FUNDING NUMBERS

6. AUTHOR(S)

Robert S. Bernard

7. PERFORMING ORGANIZATION NAME(S) AND ADDRESS(ES)

USAE Waterways Experiment Station, Hydraulics Laboratory, 3909 Halls Ferry Road, Vicksburg, MS 39180-6199

8. PERFORMING ORGANIZATION REPORT NUMBER

Technical Report HL-91-14

9. SPONSORING/MONITORING AGENCY NAME(S) AND ADDRESS(ES)

Department of the Army, Assistant Secretary of the Army (R&D), Washington, DC 20310

10. SPONSORING/MONITORING AGENCY REPORT NUMBER

11. SUPPLEMENTARY NOTES

Available from National Technical Information Service, 5285 Port Royal Road, Springfield, VA 22161.

12a. DISTRIBUTION/AVAILABILITY STATEMENT

Approved for public release; distribution is unlimited.

12b. DISTRIBUTION CODE

13. ABSTRACT *(Maximum 200 words)*

A simple adjustment is proposed that improves the predictions of the standard k-ϵ turbulence model in the presence of two-dimensional recirculating flow. An eddy Reynolds number calculated from velocity, vorticity, and eddy viscosity is introduced as a scaling parameter for reducing the decay term in the governing equation for the turbulence-energy dissipation rate. Using the adjusted k-ϵ model to compute the flow past a backstep (channel expansion), the STEMR finite-difference code gives better predictions for streamlines, velocities, and turbulence energies than it does with the standard k-ϵ model. Computed reattachment lengths compare well with experimental data for channel expansion ratios between 1 and 2.

14. SUBJECT TERMS

Incompressible flow	Recirculating flow
Numerical modeling	Turbulence modeling

15. NUMBER OF PAGES
30

16. PRICE CODE

17. SECURITY CLASSIFICATION OF REPORT	18. SECURITY CLASSIFICATION OF THIS PAGE	19. SECURITY CLASSIFICATION OF ABSTRACT	20. LIMITATION OF ABSTRACT
UNCLASSIFIED	UNCLASSIFIED		

NSN 7540-01-280-5500

Standard Form 298 (Rev 2-89)
Prescribed by ANSI Std Z39-18
298-102

PREFACE

This study was conducted from January through June 1990 by personnel of the Reservoir Water Quality Branch (RWQB), Hydraulic Structures Division (HSD), Hydraulics Laboratory (HL), US Army Engineer Waterways Experiment Station (WES). Major funding was provided by the In-House Laboratory Independent Research (ILIR) program. Additional funding was provided by the Numerical Model Maintenance Program and by the US Bureau of Reclamation through an interagency agreement for the development of a k-ϵ turbulence model.

Dr. Robert S. Bernard, RWQB, performed the research and prepared this report under the general supervision of Messrs. Frank A. Herrmann, Chief, HL; Richard A. Sager, Assistant Chief, HL; Glenn A. Pickering, Chief, HSD; and Dr. Jeffery P. Holland, Chief, RWQB. Technical assistance was provided by Mr. Herman O. Turner, RWQB, who developed pre- and postprocessors for the STREMR numerical model and executed most of the necessary computer runs on the CRAY Y-MP computer. Expert technical advice was provided by Dr. Raymond S. Chapman, private consultant to WES, who steered the author away from numerous pitfalls in turbulence modeling.

Commander and Director of WES during preparation of this report was COL Larry B. Fulton, EN. Technical Director was Dr. Robert W. Whalin.

CONTENTS

A TURBULENCE MODEL FOR RECIRCULATING FLOW

PART I: INTRODUCTION

Background

1. Although turbulence may often go unnoticed, it affects most human activities that involve air and water. If there were no such thing as turbulence, airplanes and automobiles would experience less drag, but sugar would take much longer to dissolve in coffee. In any case, when it comes to building machines whose operation depends on fluid flow, designers often have little choice but to accept and accommodate the effects of turbulence.

2. Turbulence occurs whenever there is too little viscosity to prevent small disturbances from growing and disrupting a laminar flow. Turbulent flow contains eddies of so many different sizes that a complete representation of the flow is usually impractical on a discrete grid. For some purposes, however, it is possible to approximate the behavior of the larger eddies if the influence of the smaller eddies is adequately captured by a turbulence model. In this context, the turbulence consists of all eddies that are too small to be resolved by discretization.

3. If one averages the Navier-Stokes equations over a time interval that is short compared with the periods of the large eddies, but long compared with those of the turbulence, shear stresses arise that are proportional to the time-averaged products of the fluctuating velocity components. These are called Reynolds stresses, and the process of time averaging is called Reynolds averaging. Strictly speaking, the complete turbulent velocity distribution must be known in order to calculate the Reynolds stresses exactly, but engineers have always used empirical approximations based on mean (Reynolds-averaged) velocities. The simplest of these, suggested by Boussinesq (1877), consists of supplementing the molecular viscosity with an eddy viscosity in the Newtonian expression for shear stress. Turbulence models that use this approximation are called eddy-viscosity models, and they are classified according to the manner in which they obtain the eddy viscosity from the properties of the mean flow.

4. Kinematic molecular viscosity has units of length squared divided by time, and kinematic eddy viscosity can be made proportional to any combination

of turbulence quantities that yields these same units. Algebraic eddy-viscosity models extract the necessary turbulence quantities directly from the local mean flow, without accounting for their transport by the flow itself. Since they involve no equations for turbulence transport, these models are also called zero-equation models. In contrast, one-equation models include a transport equation for one of the necessary turbulence quantities, with local algebraic approximations for the rest. Two-equation models add a transport equation for a second quantity, and so on.

5. The $k-\epsilon$ turbulence model (Launder and Spalding 1974) has become the most widely used of the two-equation eddy-viscosity models. Here the symbol k represents the turbulence energy, and ϵ the dissipation rate of the turbulence energy. Taking these as the primary turbulence quantities, each of which is governed by a transport equation, the eddy viscosity is then proportional to the ratio k^2/ϵ . By solving the two governing equations for k and ϵ along with the Reynolds-averaged equations for conservation of mass and momentum, one can obtain mean-flow approximations that are useful within certain limits. The standard $k-\epsilon$ model works fairly well for two-dimensional (2-D) flow without recirculation, as long as reliable mechanisms exist for generating shear stress and vorticity along the boundaries.

6. The adjustments needed to accommodate recirculation are quite different from those needed to resolve near-wall influences in a turbulent boundary layer (Patel, Rodi, and Scheurer 1985). That is, adjustments for recirculation offer little help in determining the point at which flow separation actually occurs, but they may be needed to avoid premature reattachment thereafter. Accurate prediction of the separation point on a smooth wall requires a grid fine enough to resolve the separating boundary layer, as well as special measures to approximate the distribution of shear stress near the wall.

Purpose and Scope

7. The present investigation concerns modifications needed to make the $k-\epsilon$ model work for 2-D recirculating flow, where the standard model may overpredict the eddy viscosity. The overprediction may arise from too much energy or from too little dissipation, and the remedy is to adjust the governing equations in a way that corrects them for recirculation but leaves them essentially unaffected for unidirectional shear flow. This is accomplished by

constructing dimensionless functions of mean-flow and turbulence quantities that can be used either for damping turbulence production or for enhancing growth of the dissipation rate. Previous efforts have employed functions of k, ϵ, and mean-flow curvature (Launder, Pridden, and Sharma 1977) to modify the standard equations. The function proposed herein employs mean-flow velocity and vorticity instead of curvature.

8. Near-wall turbulence correction and boundary layer separation lie outside the scope of the study reported here, which is concerned mainly with flow behavior after separation. Fortunately, computed flows and real turbulent flows separate whenever they encounter sharp corners, so there is no difficulty in predicting separation points for sharp-cornered boundaries. Given the separation point, a discrete flow-solver with an adequate turbulence model should be able to predict the downstream reattachment point and the predominant features of the recirculating flow, at least for simple geometries.

9. Part II of this report outlines the governing equations for the mean flow and the standard turbulence model, and Part III discusses the associated boundary conditions. Part IV offers proposed modifications to the k-ϵ model; Part V describes the numerical algorithms used to discretize and solve the equations; Part VI enumerates the reasons for choosing the backstep as a test problem; Part VII presents comparisons of mean-flow computations with experimental results; and Part VIII sets forth conclusions and recommendations.

PART II: GOVERNING EQUATIONS

10. The governing equations for the mean flow are the Reynolds-averaged Navier-Stokes equations. For 2-D incompressible flow, these are the equations for conservation of mass and momentum, given respectively by

$$\nabla \cdot \underline{u} = 0 \tag{1}$$

$$\underline{u}_t + \underline{u} \cdot \nabla \underline{u} = \underline{T} - \frac{\nabla p}{\rho} \tag{2}$$

where

- ∇ = gradient operator
- $\underline{u}$ = vector velocity
- t = time
- $\underline{T}$ = divergence of the Reynolds-averaged stress tensor
- p = pressure
- ρ = density

An underbar indicates vectors and a subscript t indicates a time derivative. The cartesian x- and y-components of $\underline{T}$ are, respectively,

$$T_1 = \nu \nabla^2 u + 2\nu_x u_x + \nu_y (u_y + v_x) \tag{3}$$

$$T_2 = \nu \nabla^2 v + 2\nu_y v_y + \nu_x (v_x + u_y) \tag{4}$$

where

- ν = eddy viscosity
- u, v = x- and y-components of $\underline{u}$
- x, y = cartesian coordinates

and the subscripts x and y indicate spatial derivatives. (Molecular viscosity is neglected in Equations 3 and 4.) The eddy viscosity is related to the turbulence energy k and the turbulence dissipation rate ϵ by

$$\nu = C_\nu \frac{k^2}{\epsilon} \tag{5}$$

where C_ν is a dimensionless empirical coefficient.

11. The governing equations for k and ϵ are semi-empirical transport equations, each of which has the form

Advection = Production − Dissipation + Diffusion

In this context, advection means transport by the mean flow; production means creation from the large eddies; dissipation means frictional loss through the small eddies; and diffusion means the spreading that occurs because of eddy viscosity. In the standard $k-\epsilon$ model, the governing equations are

$$k_t + \underline{u} \cdot \nabla k = \nu \Gamma - \epsilon + \sigma_k^{-1} \nabla \cdot (\nu \nabla k) \tag{6}$$

$$\epsilon_t + \underline{u} \cdot \nabla \epsilon = C_1 \nu \Gamma \frac{\epsilon}{k} - C_2 \frac{\epsilon^2}{k} + \sigma_\epsilon^{-1} \nabla \cdot (\nu \nabla \epsilon) \tag{7}$$

In each case, the first term on the right is the production term, which is proportional to

$$\Gamma = 2\left(u_x^2 + v_y^2\right) + \left(u_y + v_x\right)^2 \tag{8}$$

The second term on the right in Equations 6 and 7 is the dissipation term, and the third term is the diffusion term. The standard set of dimensionless empirical coefficients (Launder and Spalding 1974) is

$$\begin{aligned} C_\nu &= 0.09 \\ C_1 &= 1.44 \\ C_2 &= 1.92 \\ \sigma_k &= 1.0 \\ \sigma_\epsilon &= 1.3 \end{aligned}$$

12. With suitable boundary conditions for u , v , p , k , and ϵ , Equations 1, 2, 6, and 7 are sufficient for calculating 2-D flow within the limitations of the $k-\epsilon$ turbulence model. The STREMR finite-difference code (Bernard 1989) was used to discretize and solve the governing equations for the work reported here. Starting with potential flow for the initial velocity and small uniform values for the initial turbulence quantities, STREMR obtains steady-state solutions (if they exist) by marching forward in time.

PART III: BOUNDARY CONDITIONS

13. In the STREMR code, velocity components normal to the boundaries are held fixed for inlets (nonzero mass inflow) and solid walls (zero mass inflow/outflow) and computed by a discrete radiation condition for outlets (nonzero mass outflow). The total flow rate remains constant, as do the individual flow rates through each inlet and outlet. In a given time-step, the velocity normal to any boundary segment is either constant (for inlets and solid walls) or determined by neighboring velocities in the previous time-step (for outlets). STREMR uses a staggered marker-and-cell grid, with mass flux components defined on cell faces and pressures defined at cell centers. This grid arrangement, along with the specification of all boundary-normal mass fluxes at the beginning of each time-step, allows the normal component of the pressure gradient to be set to zero on all boundaries.

14. In principle, both the normal and tangential components of velocity should be zero on all solid boundaries. For the normal component this means no mass flux through the boundary, and the resulting effect on the rest of the flow can be obtained without special refinement of the grid. In the case of the tangential component, however, the velocity gradient may be so sharp that accurate resolution becomes difficult near the boundary itself. Thus, even with zero tangential velocity specified on a wall, the discrete solution may still fail to approximate the near-wall velocity distribution and its effect on the rest of the flow.

15. Solid walls pose more of a problem than merely that of grid resolution. Since turbulence dies off very near a wall, turbulence models must also account for wall proximity. If this is not adequately done, a flow calculation may be invalid whether or not the grid is fine enough to resolve the velocity gradient. In general, wall effects have to be accommodated either by using special near-wall turbulence models (Patel, Rodi, and Scheurer 1985) or by using empirical formulas to estimate near-wall turbulence quantities (Rodi 1980).

16. Near-wall turbulence models are usually adaptations of familiar models like the k-ϵ model, in which coefficients and functions are modified or added with decreasing distance from a wall. In a boundary layer or other wall-bound shear flow, their purpose is to represent the viscous sublayer, which is so thin and so close to the wall that the shear stress created by

molecular viscosity ν_m is comparable with that created by turbulence. In a boundary layer with no pressure gradient, the viscous sublayer is said to lie in the range

$$0 \leq y^+ \leq 10 \tag{9}$$

where y^+ is the dimensionless normal distance from a horizontal wall,

$$y^+ = \frac{u_* y}{\nu_m} \tag{10}$$

and u_* is the friction velocity. This latter quantity is related to the tangential shear stress τ_w on the wall by

$$\tau_w = \rho u_*^2 \tag{11}$$

and the wall shear stress is given in terms of the molecular viscosity and the velocity distribution by

$$\tau_w = \rho \nu_m \frac{\partial u}{\partial y} \tag{12}$$

with the velocity derivative evaluated <u>at</u> the wall $(y = 0)$. In order to calculate τ_w from scratch, one must use a near-wall turbulence model, along with the mean-flow equations, to calculate the velocity distribution imposed on the viscous sublayer by the no-slip condition. Otherwise it is necessary to assume a near-wall velocity distribution and, by implication, a value for the wall shear stress.

17. Perhaps the most commonly used near-wall velocity profile is the logarithmic law of the wall,

$$\frac{u}{u_*} = \frac{1}{\kappa} \ln (Ey^+) \tag{13}$$

where κ is von Karman's constant (about 0.418), and E is a roughness factor (about 9.75 for hydraulically smooth walls). This empirical formula provides a convenient relation between friction velocity, local flow velocity, molecular viscosity, and wall roughness. It is reliable in the range $30 < y^+ < 150$ when there is no pressure gradient, but it has often been used to give a rough approximation for u_* even when there <u>is</u> a pressure gradient (Rodi

1980). There are also modified versions of the law of the wall that take the pressure gradient into account, but they offer little improvement over Equation 13 for separating or recirculating flow (Chen and Patel 1988).

18. In general, near-wall flow cannot be calculated independently of the flow at large, because the interaction of the two usually determines the location of separation and reattachment points. Wherever there is a sharp convex corner, however, the flow will always separate, and the downstream recirculating flow may be only weakly dependent on near-wall conditions for some distance prior to reattachment. In these circumstances it may be possible to model the effect of turbulence in the recirculating flow, even when the wall shear stress is poorly approximated.

19. In the present work, the standard law of the wall (Equation 13) provides the needed relation between friction velocity and flow velocity adjacent to solid walls. In addition to a nonzero value for the shear stress on the wall, this gives boundary values for the turbulence energy,

$$k_w = C_\nu^{-1/2} u_*^2 \tag{14}$$

and also the turbulence dissipation rate,

$$\epsilon_w = \frac{u_*^3}{\kappa y} \tag{15}$$

These equations represent token approximations for the actual boundary conditions, but they are acceptable if the flow separates at a sharp corner and recirculates strongly thereafter.

20. Small, fixed values of k and ϵ are specified along inlets, and Neumann conditions (zero normal derivatives) are imposed on k and ϵ along outlets and slip boundaries. This combination of boundary conditions (including the law of the wall) helps to preserve numerical stability and keeps the computed solution from drifting.

PART IV: MODIFICATIONS TO THE STANDARD MODEL

21. Various authors (e.g., Chapman and Kuo 1985) have reported that the $k-\epsilon$ model underpredicts reattachment lengths for separated flow, but the reason for this underprediction is not clear. One possibility is that the standard model is unsuitable for recirculating flow because it assumes the normal components of the Reynolds stress tensor to be isotropic. Indeed, in strongly three-dimensional (3-D) flow, anisotropic normal stresses do induce secondary (helical) mean currents that cannot be predicted with isotropy alone. In two dimensions, however, 3-D secondary currents exist only as part of the turbulence, and normal-stress anisotropy may or may not have a strong influence on the mean flow. Speziale (1987) has developed a nonlinear $k-\epsilon$ model that includes anisotropic normal stresses and gives somewhat improved predictions for 2-D and 3-D recirculating flow.

22. Rodi (1980) has observed that the standard model breaks down with large departures from equilibrium; i.e., when the rate of turbulence energy production greatly exceeds the rate of dissipation, and vice versa. To improve nonequilibrium flow predictions, Rodi has proposed an empirical correction factor for the eddy viscosity, based on the average ratio of production to dissipation for the mean flow. The use of averaging does not seem appropriate for recirculating flow, however, because the ratio of production to dissipation can change abruptly with position.

23. Whatever the reason, the standard $k-\epsilon$ model seems consistently to underpredict reattachment lengths for backsteps. The amount of discrepancy varies somewhat with channel width and with the numerical scheme used for calculation, but the model invariably produces too much eddy viscosity in the recirculating zone. To counter this tendency, one then seeks an empirical adjustment that reduces the viscosity for separated flow, but not necessarily for unseparated flow. The adjustment should rely on a scaling parameter that is some dimensionless combination of turbulence and mean-flow quantities, which should be easy to implement in the standard $k-\epsilon$ equations.

24. Drawing on an analogy between buoyancy and curvature proposed by Bradshaw (1969), Launder, Priddin, and Sharma (1977) have formulated an adjustment to the $k-\epsilon$ model based on the streamline radius of curvature. This correction, known as the LPS correction, was intended for boundary layers; but it has also been used for recirculating flow by Durst and Rastogi (1980) and

by Tingsanchali and Maheswaran (1990) among others. In this procedure, one first defines a turbulent Richardson number (based on curvature instead of buoyancy),

$$R_i = \frac{k^2}{\epsilon^2} \frac{(u^2 + v^2)^{1/2}}{r} (v_x - u_y) \tag{16}$$

where r is the streamline radius of curvature, given by

$$\frac{1}{r} = \frac{uv(v_y - u_x) + u^2 v_x - v^2 u_y}{(u^2 + v^2)^{3/2}} \tag{17}$$

The Richardson number is then used to obtain a curvature-corrected value C_2' for the coefficient C_2,

$$C_2' = C_2(1 - C_c R_i) \tag{18}$$

where C_c is a dimensionless curvature correction coefficient.

25. With Equation 18, a positive value for R_i reduces the decay rate for the dissipation, which increases the dissipation rate and reduces the turbulence energy. A negative value has the opposite effect.

26. Although the LPS correction improves predictions in some cases, it is not universally satisfactory for 2-D calculations (Rodi and Scheurer 1983). Apparently something more than curvature alone is needed for improving the k-ϵ model in two dimensions. As an alternative parameter, consider the eddy Reynolds number R_E defined as follows:

$$R_E = (u^2 + v^2)^{1/2} \frac{\delta_E}{\nu} \tag{19}$$

The length scale δ_E is obtained from the mean-flow velocity and vorticity through the relation

$$\delta_E = \frac{(u^2 + v^2)^{1/2}}{|v_x - u_y|} \tag{20}$$

When Equations 19 and 20 are combined with Equation 5, the expression for R_E becomes

$$R_E = \frac{(u^2 + v^2)\,\epsilon}{C_\nu k^2\, |v_x - u_y|} \tag{21}$$

This quantity is a convenient parameter for tuning the production and dissipation of turbulence, because it increases with velocity and dissipation rate, but decreases with energy and with energy production (which increases roughly as the square of vorticity).

27. In the range of y^+ associated with the law of the wall, R_E takes values in excess of 30. If the k-ϵ model is to retain its applicability for wall-bound shear flows, any correction factor based on the eddy Reynolds number should approach unity at values of R_E near 30 or more. With this in mind, consider the following adjustment for the coefficient C_2 in the standard model:

$$C_2' = C_1 + \frac{C_2 - C_1}{1 + R_C^3/R_E^3} \tag{22}$$

Equation 22 exhibits the desired behavior for $R_E > 30$ as long as the empirical coefficient R_C is given values of about 10 or less. In this context, R_C represents a cutoff value for R_E, below which C_2' rapidly approaches C_1. Above R_C, the altered coefficient C_2' gradually approaches the standard C_2.

28. For future reference, Equation 22 will be called the eddy Reynolds number (ERN) correction for the k-ϵ turbulence model. Aside from their dependence on vorticity and streamline curvature, the main qualitative difference between the ERN and LPS corrections is that LPS may either increase or decrease the decay rate for dissipation, while ERN can only decrease it. These adjustments represent two of many plausible corrections that one might propose for the standard model. Both are easy to implement, and neither adds significantly to the computer time required for the standard model.

PART V: NUMERICAL ALGORITHMS

29. The STREMR computer code ordinarily uses only the MacCormack predictor-corrector scheme (MacCormack 1969; Bernard 1989) to solve the momentum equation (Equation 2), but for this study a special version of the code was set up to use an upwind predictor-corrector scheme as well. To discretize the advective terms in Equation 2, the MacCormack solver uses forward spatial differencing in the predictor phase of each time-step, and backward differencing in the corrector (or vice versa). The upwind solver uses two-point upwind differencing in both the predictor and corrector phases. The MacCormack scheme is second-order accurate (at best) in space, while the upwind scheme is only first-order accurate. By running the same calculations with these two different numerical methods, one can roughly ascertain the degree to which model predictions may be algorithm dependent.

30. Both versions of STREMR use a single-step (predictor phase only) upwind scheme for solving the k-ϵ equations, regardless of the method employed for the momentum equation. The code begins with potential flow for the mean flow and with small, uniform values for k and ϵ. It then marches through time toward a steady state (if one exists). The same time-step size is used for every cell on the grid, but this is updated every 10 time-steps to the maximum value allowed by numerical stability considerations.

31. In each time-step, the eddy viscosity is first calculated using existing values of k and ϵ. This viscosity is then used to compute new values for u, v, k, and ϵ. The pressure needed to maintain conservation of mass is obtained from the solution to a Poisson equation in each predictor and corrector phase.

PART VI: TEST PROBLEM

32. The flow past a backstep (abrupt channel expansion) has been chosen to test the proposed ERN correction for the k-ϵ turbulence model. In selecting a test problem, one seeks to eliminate or reduce the influence of competing mechanisms that create confusion and render calculations inconclusive. In the case of the backstep, the flow is essentially unidirectional and parallel to the wall when it separates at the channel expansion, regardless of the upstream velocity distribution.

33. The flow downstream of a backstep is not completely insensitive to upstream conditions, but it is less sensitive than that for a forestep (abrupt contraction) or a block (contraction followed by expansion). With the forestep and the block, the upstream velocity governs the flow separation angle at the contraction, which likewise governs the recirculating flow downstream. Turbulence model tests for these configurations will be inconclusive unless both the upstream and downstream flow can be accurately predicted from scratch. The backstep eliminates much of the upstream dependence, and this makes it more convenient for model tests in recirculating flow.

34. After the flow separates at the corner, it recirculates for some distance in the wake of the backstep. At some point, however, the flow again becomes unidirectional (no backflow), and this is called the point of reattachment. The channel expansion ratio h_2/h_1 is the main parameter that controls the reattachment point, where h_1 and h_2 are the depths upstream and downstream of the expansion in the xy-plane (Figure 1). The step height h is the difference between h_2 and h_1:

$$h = h_2 - h_1 \tag{23}$$

If horizontal position x is measured from the backstep, and x_R is the reattachment length, then x_R/h increases with h_2/h_1. Although Reynolds number also has some influence on reattachment, it is less important than the expansion ratio (Durst and Tropea 1981).

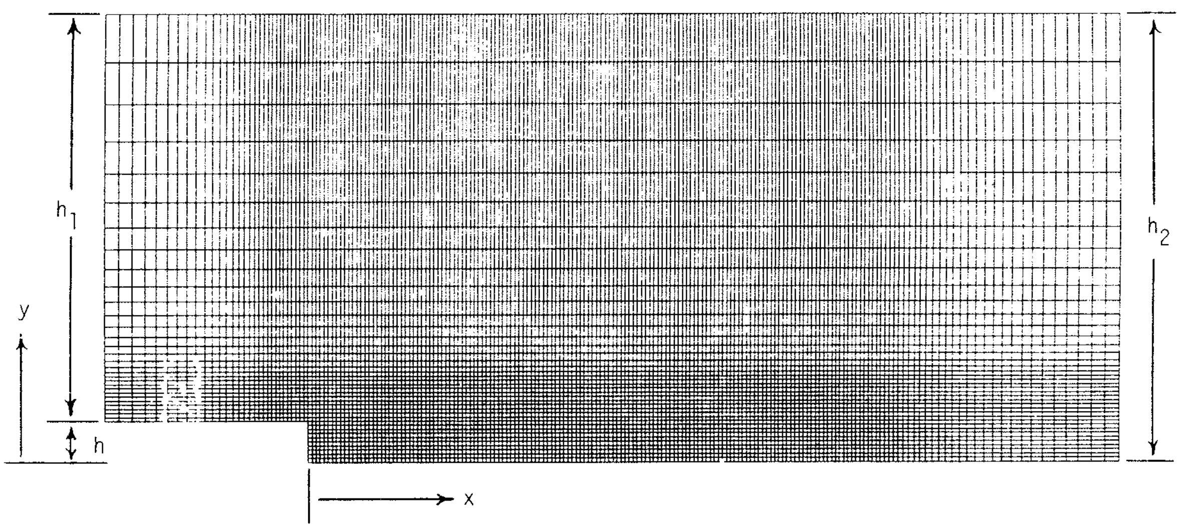

Figure 1. Computational grid for channel expansion with $h_2/h_1 = 1.1$

PART VII: COMPUTED RESULTS

35. STREMR calculations were executed for uniform inflow into a channel expansion (Figure 1) with the law of the wall imposed on the lower (backstep) boundary and perfect slip on the upper (symmetry) boundary. The computational domain was a rectangle with a length of 30h and a width of 11h, which was divided into a grid with 200 spaces in the x-direction and 40 spaces in the y-direction. Channels with different expansion ratios were created by blocking out rows of cells along the upper boundary of the rectangle. Although the grid spacing was uneven far from the backstep, the grid cells in the recirculation zone were uniformly square ($\Delta x = \Delta y = h/10$) in all cases. The expansion ratio was varied from 1.1 to 2.0, but the conventional (molecular) Reynolds number was held fixed at $R_m = 5 \times 10^4$, where

$$R_m = \frac{u_0 h}{\nu_m} \tag{24}$$

and u_0 is the inflow velocity.

36. Figure 2 shows streamlines computed for an expansion ratio of 1.48 with the MacCormack flow-solver and the ERN turbulence correction. Note that for $R_c = 0$ the ERN correction reduces to the standard $k-\epsilon$ model. It is evident from these results that the adjusted turbulence model predicts greater reattachment lengths and stronger recirculation than the standard model.

37. In Figure 3 the turbulence-energy predictions for $h_2/h_1 = 1.48$ are compared with the measurements made by Kim, Kline, and Johnston (1980) for $h_2/h_1 = 1.50$. The ERN correction ($R_c = 5$) produces less energy than the standard model ($R_c = 0$) upstream of the reattachment point ($x_R/h \approx 7.5$), where the ERN predictions are more nearly in agreement with the experimental data. Downstream of reattachment, the predicted energies are almost the same. A similar comparison with the velocity data (Figure 4) shows that the ERN correction yields a stronger and longer backflow than the standard model, and that the ERN predictions are generally in better agreement with the measurements.

38. The agreement between calculation and observation in Figures 3 and 4 is about as good as can be expected with the MacCormack solver and the ERN turbulence correction; it is unlikely that before-the-fact predictions will be

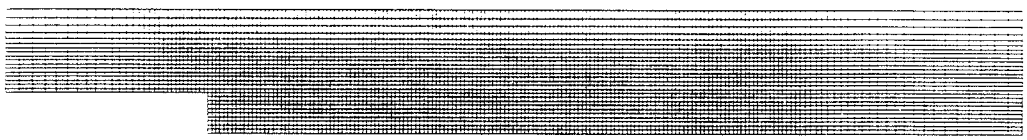

a. Computational grid

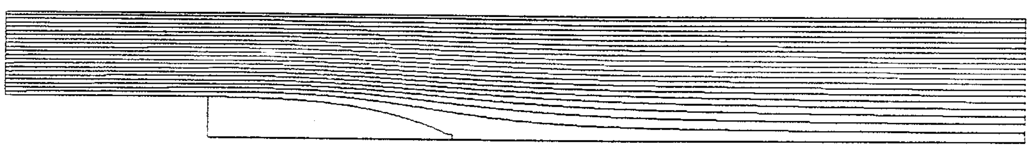

b. Standard model (R_c = 0)

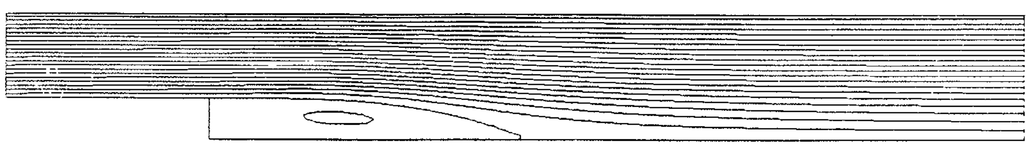

c. ERN correction (R_c = 5)

Figure 2. Streamlines computed with MacCormack flow-solver for channel expansion with h_2/h_1 = 1.48

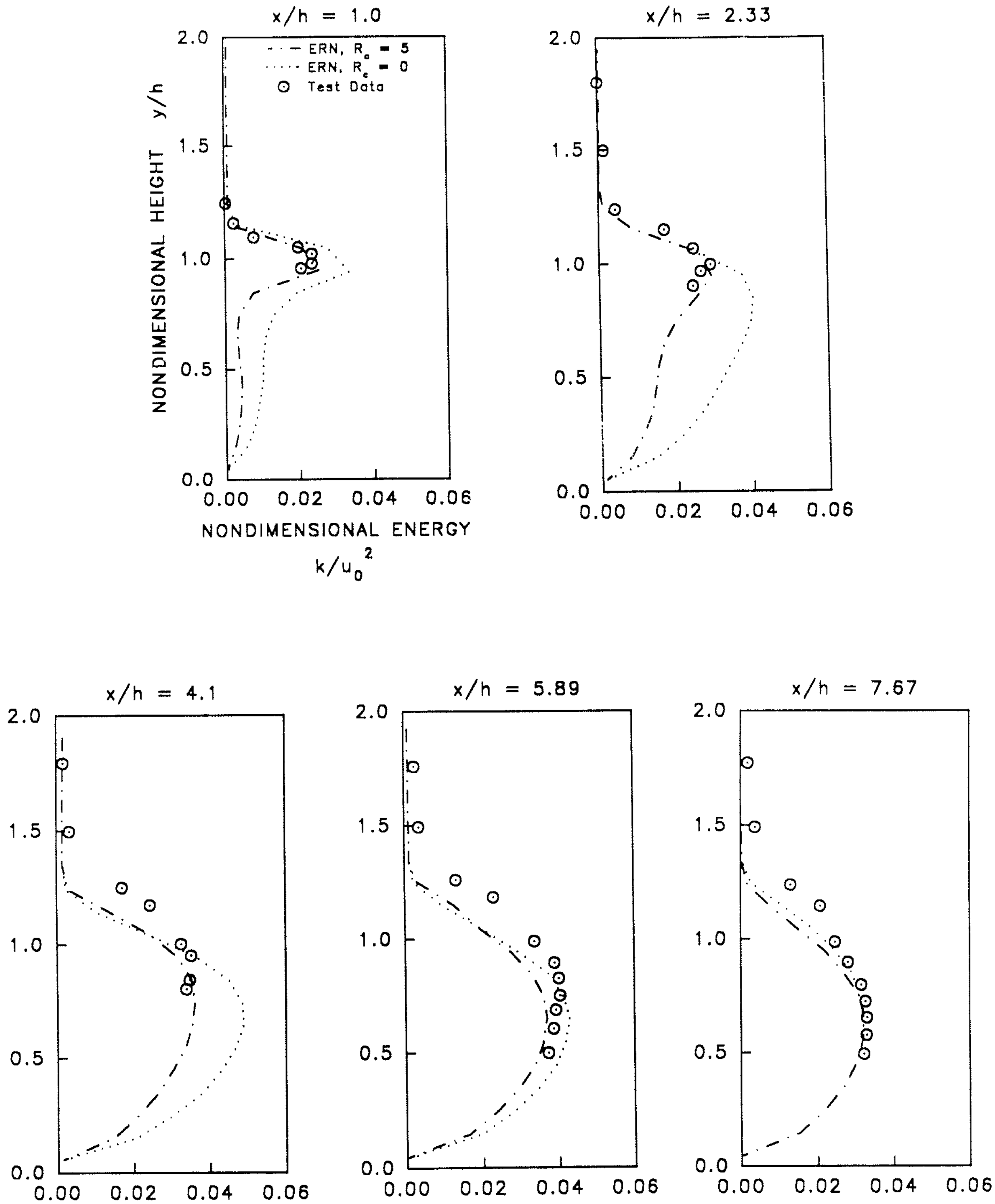

Figure 3. Comparison of experimental data (h_2/h_1 = 1.5) with turbulence energies computed by MacCormack flow-solver with standard model (R_c = 0) and with ERN correction (R_c = 5)

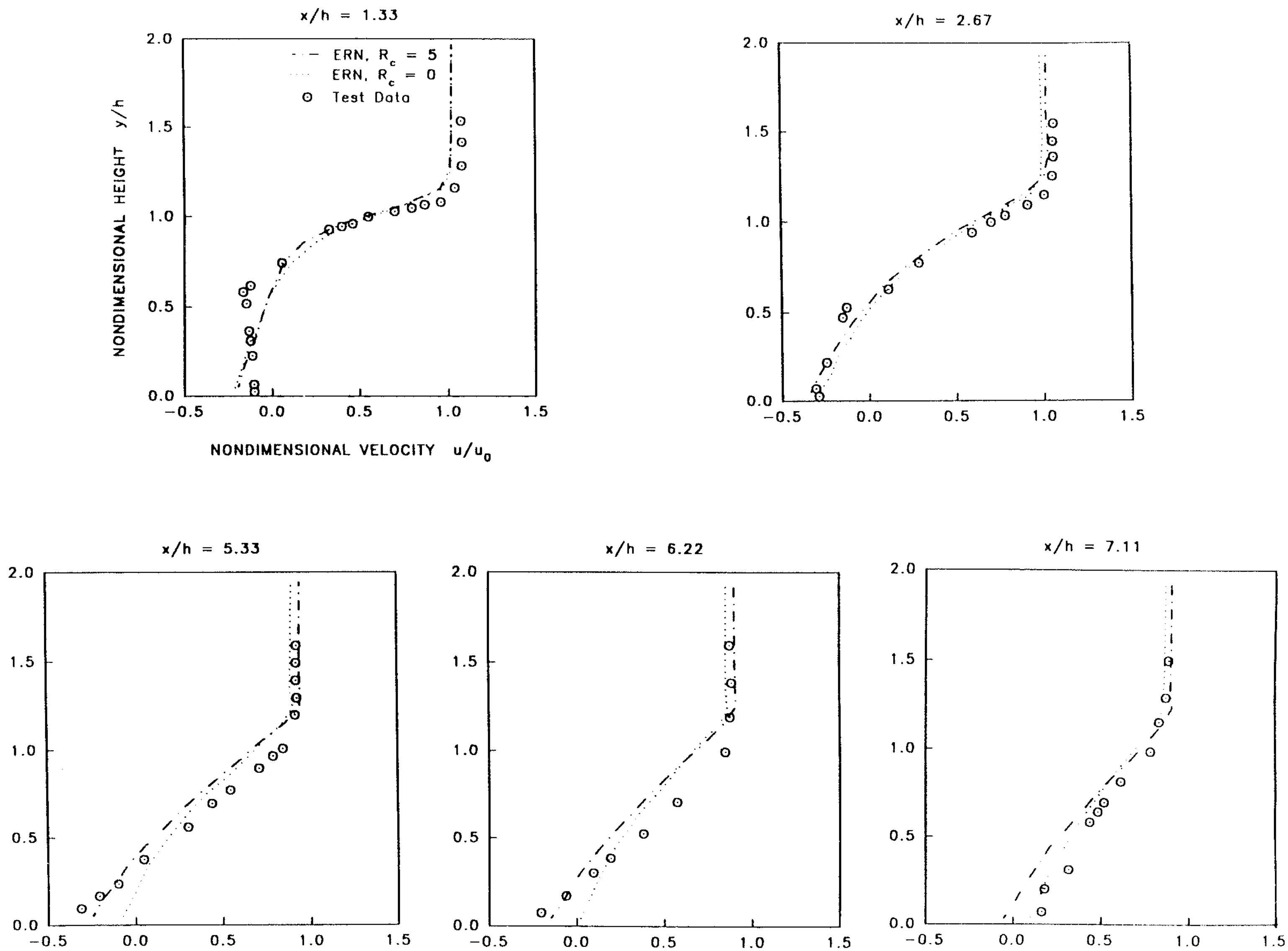

Figure 4. Comparison of experimental data ($h_2/h_1 = 1.5$) with velocities computed by MacCormack flow-solver with standard model ($R_C = 0$) and with ERN correction ($R_C = 5$)

much better than the results shown here. It may often be possible to find a value for R_C that forces agreement for a specific case after the fact (as was done here), but that does not imply that the same will be achieved in general. Thus, it is important to investigate the performance of the model for other expansion ratios, and also the extent to which predictions may vary with an alternative numerical scheme and turbulence correction.

39. Durst and Tropea (1981) have compiled experimental measurements of x_R/h from fifteen different sources (including their own work) for $1 < h_2/h_1 \leq 2$ with Reynolds numbers in the range $2.5 \times 10^3 \leq R_m \leq 1.3 \times 10^5$. These are the data with which model results for reattachment length will be compared.

40. Identical sets of calculations were done for each of four possible combinations of flow-solver (MacCormack or upwind) and turbulence correction (ERN or LPS). The predicted reattachment lengths x_R are compared with experimental data in Figures 5 and 6. Note that the turbulence model reduces to the standard k-ϵ model when $R_C = 0$ with the ERN correction, and when $C_c = 0$ with the LPS correction.

41. The standard model ($R_C = 0$) consistently underpredicts the reattachment length with both flow-solvers, but the underprediction is greater with the upwind scheme. This is to be expected, because the MacCormack solver produces less numerical diffusion than does the upwind. Even so, the upwind does not fare badly in comparison with the MacCormack, except perhaps for expansion ratios near unity.

42. The ERN correction pushes the predictions in the right direction, achieving the best overall results for $R_C \approx 5$ with the MacCormack scheme (Figure 5). The end points of the predicted curve are about right, but the slope is rather different from that indicated by the experiments for expansion ratios near unity. The observed reattachment lengths climb sharply in the range $1.1 < h_2/h_1 < 1.3$ and gently otherwise. The predicted values, on the contrary, exhibit a gradual increase with expansion ratio in the range between 1.1 and 2.0 . This discrepancy may reflect some inconsistency in the experimental data, or (more likely) it may imply that R_E is not a perfectly satisfactory parameter for adjusting the turbulence model.

43. The predicted results with the LPS correction (Figure 6) are generally worse than those with the ERN correction. With the upwind flow-solver, the LPS calculations were numerically stable for all values of C_c in the

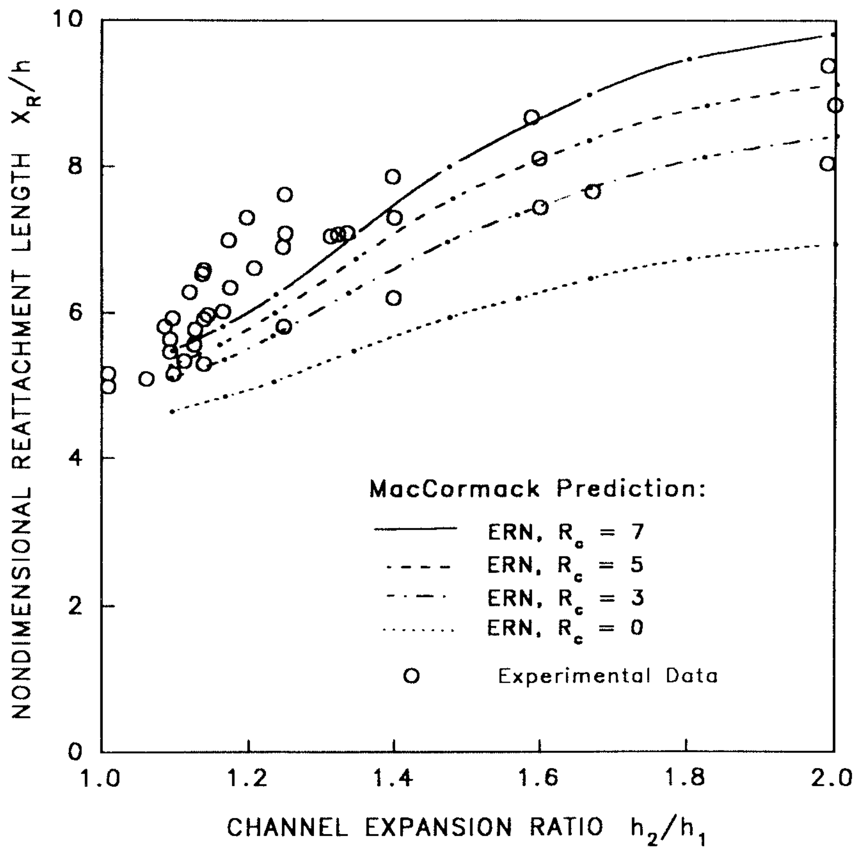

a. MacCormack flow-solver

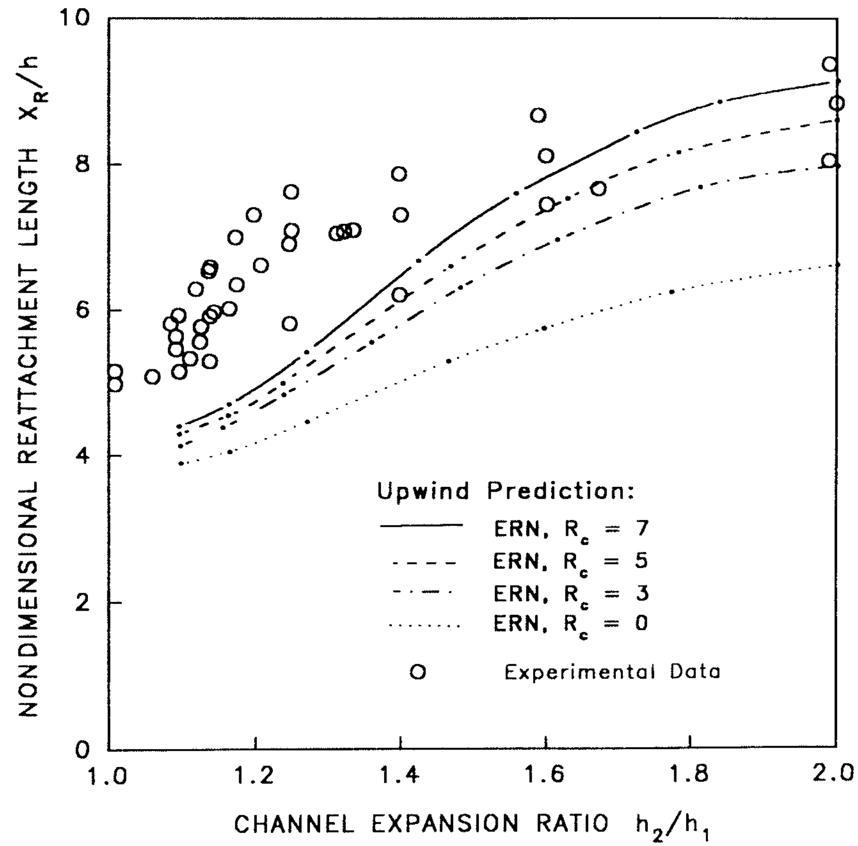

b. Upwind flow-solver

Figure 5. Comparison of experimental data with reattachment lengths computed by MacCormack and upwind flow-solvers with ERN turbulence correction

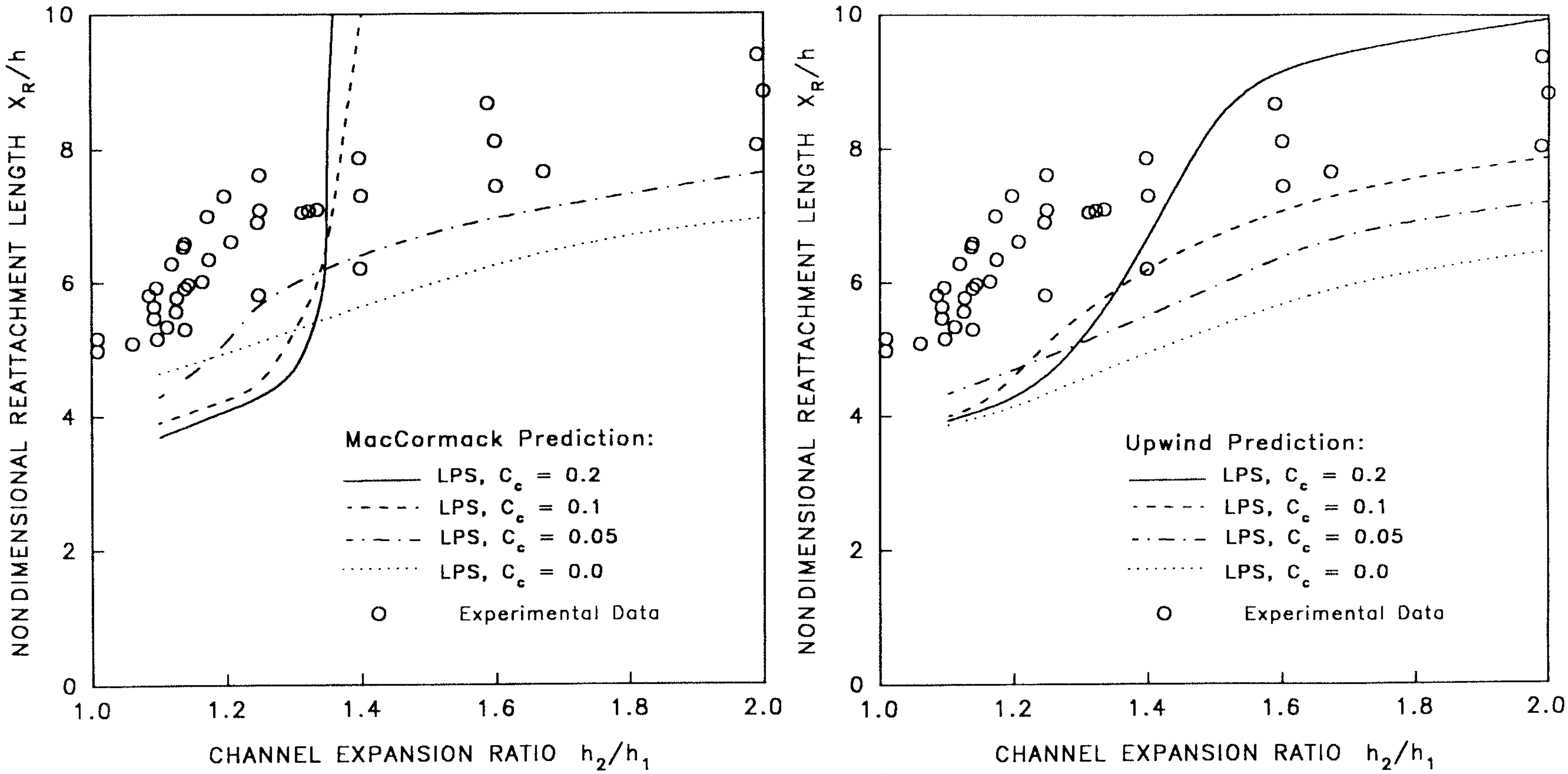

a. MacCormack flow-solver

b. Upwind flow-solver

Figure 6. Comparison of experimental data with reattachment lengths computed by MacCormack and upwind flow-solvers with LPS turbulence correction

range $0.0 < C_c < 0.2$ and for all expansion ratios in the range $1.1 \leq h_2/h_1 \leq 2.0$. On the other hand, with the MacCormack flow-solver (Figure 6a) these calculations failed to converge for $h_2/h_1 > 1.4$ when C_c was 0.1 or greater. Even with the upwind scheme, the LPS reattachment curves (Figure 6b) are less in agreement with the data than are the ERN curves (Figure 5b).

PART VIII: CONCLUSION

44. The proposed ERN (eddy Reynolds number) correction reduces the turbulence energy and eddy viscosity generated by the standard $k-\epsilon$ model in the presence of recirculation. This consistently improves flow predictions for backsteps (channel expansions) with expansion ratios between 1 and 2, even though the computed reattachment lengths do not follow precisely the curve outlined by the experimental data.

45. The LPS (curvature) correction proposed by Launder, Priddin, and Sharma (1977) does not work in general for recirculating flow. The upwind flow-solver converges with the LPS correction (Equation 18), but the predicted variation of reattachment length with channel expansion ratio has the wrong shape. The MacCormack solver converges with LPS when $C_c = 0.05$ or less, but it may encounter difficulties with convergence or stability when $C_c = 0.10$ or more. In any case, to tune the ERN correction (Equation 22) properly for the $k-\epsilon$ model, one should always use experimental data like those of Durst and Tropea (1981) to help find R_c for the particular numerical flow-solver being used. No two algorithms will give precisely the same results, and sometimes the disparity in predictions can be significant.

46. The ERN turbulence correction should be viewed as a tentative adjustment which is helpful in two dimensions, but not necessarily in three. This is not to say that the ERN is without merit as a scaling parameter in three dimensions, but that other parameters may be necessary along with a more advanced turbulence model than an eddy-viscosity model. Even in two dimensions, the ERN correction merely represents an empirical extension that improves predictions; it does not offer a better understanding of the turbulence itself.

47. Within the limitations of 2-D flow, there still remains the problem of resolving near-wall effects well enough that reliable predictions can be made for separation and reattachment on boundaries of arbitrary shape. Once this problem has been adequately solved, the $k-\epsilon$ model may prove quite useful for general hydrodynamic and aerodynamic applications in two dimensions.

REFERENCES

Bernard, R. S. 1989 (Mar). "Explicit Numerical Algorithm for Modeling Incompressible Approach Flow," Technical Report REMR-HY-5, US Army Engineer Waterways Experiment Station, Vicksburg, MS.

Boussinesq, J. 1877. "Essai Sur La Theorie Des Eaux Courantes," Mem. Presentes Acad. Sci., Paris, Vol 23, p 46.

Bradshaw, P. 1969. "The Analogy Between Streamline Curvature and Buoyancy in Turbulent Shear Flow," Journal of Fluid Mechanics, Vol 36, No. 1, pp 177-191.

Chapman, R. S., and Kuo, C. Y. 1985. "Application of the Two-Equation k-ϵ Turbulence Model to a Two-Dimensional, Steady, Free Surface Flow Problem with Separation," International Journal for Numerical Methods in Fluids, Vol 5, pp 257-268.

Chen, H. C., and Patel, V. C. 1988. "Near-Wall Turbulence Models for Complex Flows Including Separation," AIAA Journal, Vol 26, No. 6, pp 641-648.

Durst, F., and Rastogi, A. K. 1980. "Turbulent Flow Over Two-Dimensional Fences," Turbulent Shear Flows, Vol 2, Springer-Verlag, New York, pp 218-232.

Durst, F., and Tropea, C. 1981. "Turbulent, Backward-Facing Step Flows in Two-Dimensional Ducts and Channels," Proceedings of the Third Symposium on Turbulent Shear Flows, 9-11 September 1981, University of California, Davis, CA.

Kim, J., Kline, S. J., and Johnston, J. P. 1980. "Investigation of a Reattaching Turbulent Shear Layer: Flow over a Backward-Facing Step," Journal of Fluid Engineering, Transactions of the American Society of Mechanical Engineers, Vol 102, pp 302-308.

Launder, B. E., and Spalding, D. B. 1974. "The Numerical Calculation of Turbulent Flows," Computer Methods in Applied Mechanics and Engineering, Vol 3, pp 269-289.

Launder, B. E., Priddin, C. H., and Sharma, B. I. 1977. "The Calculation of Turbulent Boundary Layers on Spinning and Curved Surfaces," Journal of Fluid Engineering, Transactions of the American Society of Mechanical Engineers, Series D, Vol 99, pp 231-238.

MacCormack, R. W., 1969. "The Effect of Viscosity in Hypervelocity Impact Cratering," AIAA Paper 69-354, American Institute of Aeronautics and Astronautics, Cincinnati, OH.

Patel, V. C., Rodi, W., and Scheurer, G. 1985. "Turbulence Models for Near-Wall and Low Reynolds Number Flows: A Review," AIAA Journal, Vol 23, No. 9, pp 1308-1319.

Rodi, W. 1980 (Jun). "Turbulence Models and Their Application in Hydraulics - A State of the Art Review," State-of-the-Art Paper, International

Association for Hydraulic Research, Delft, The Netherlands.

Rodi, W., and Scheurer, G. 1983. "Calculation of Curved Shear Layers with Two-Equation Turbulence Models," Physics of Fluids, Vol 26, No. 6, pp 1422-1436.

Speziale, C. G. 1987. "On Nonlinear K-ℓ and K-ϵ Models of Turbulence," Journal of Fluid Mechanics, Vol 178, pp 459-475.

Tingsanchali, T., and Maheswaran, S. 1990. "2-D Depth-Averaged Flow Computation near Groyne," Journal of Hydraulic Engineering, Vol 16, No. 1, pp 71-86.